

MedChemComm

Accepted Manuscript



This is an *Accepted Manuscript*, which has been through the Royal Society of Chemistry peer review process and has been accepted for publication.

Accepted Manuscripts are published online shortly after acceptance, before technical editing, formatting and proof reading. Using this free service, authors can make their results available to the community, in citable form, before we publish the edited article. We will replace this *Accepted Manuscript* with the edited and formatted *Advance Article* as soon as it is available.

You can find more information about *Accepted Manuscripts* in the [Information for Authors](#).

Please note that technical editing may introduce minor changes to the text and/or graphics, which may alter content. The journal's standard [Terms & Conditions](#) and the [Ethical guidelines](#) still apply. In no event shall the Royal Society of Chemistry be held responsible for any errors or omissions in this *Accepted Manuscript* or any consequences arising from the use of any information it contains.



www.rsc.org/medchemcomm

Abbreviations:

SAR, Structure-Activity Relationship; CAA, cationic anthraquinone analog; NCI, National Cancer Institute; ROS, reactive oxygen species; GSH, glutathione; FDA, U.S. Food and Drug Administration; MIC, minimum inhibitory concentration; MTT, 3-(4,5-methylthiazol-2-yl)-2,5-diphenyltetrazolium bromide; A/PI, Annexin-V/Propidium Iodide; FITC, fluorescein isothiocyanate; $\Delta\Psi_m$, mitochondrial membrane potential; DAPI, 4',6-diamidino-2-phenylindole; GMP, guanosine mono-phosphate; TBAP, tetrabutylammonium hexafluorophosphate; $E_{1/2}$, Half wave potential; DCFH-DA, fluorescent dichloro-dihydro-fluorescein diacetate.

ABSTRACT

Previously we reported synthesis and structure-activity relationship (SAR) study of a series of novel 4,9-dioxo-4,9-dihydro-1*H*-naphtho[2,3-*d*][1,2,3]triazol-3-ium salts, which had very potent anti-proliferative activities (low μM to nM GI_{50}) against a broad range of cancer cells. These compounds, which can be viewed as cationic anthraquinone analogs (CAA's), are selective against cancer cells over bacteria or fungi as compared to the antibacterial CAA's that have also been reported by our group. Herein, we report the mode of action study of CAA's, which reveals that these compounds trigger apoptosis by generating extensive reactive oxygen species (ROS). The generation of extensive ROS species causes oxidative stress, decrease in mitochondrial membrane potential, depletion of glutathione (GSH), and release of caspase-3; which ultimately kills cancer cells by programmed apoptosis. Furthermore, we have also showed that CAA's possess activity 8-fold higher against A549 cell vs non-cancerous MRC-5 cell.

INTRODUCTION

The development of novel antitumor agents has long been the focused area in cancer chemotherapy.¹ Molecules bearing quinone motifs have attracted great interest due to their potential uses as cancer chemotherapeutics.² Several anticancer drugs containing quinone motif have been approved by U.S. Food and Drug Administration (FDA) for clinical use, e.g. daunomycin, doxorubicin, mitomycin C, and mitoxanthrone (Figure 1A). Natural compounds containing quinone motif such as cribrostatain, streptonigrin, and β -lapachone are further being studied for their anti-cancer activities,^{3,4} of which streptonigrin and β -lapachone are already being used as an experimental drugs. Our laboratory is dedicated to synthesizing small molecules containing 1,4-naphthoquinone or other heterocyclic motifs as an antimicrobial or as an anticancer drug. These compounds can be prepared in 2-3 steps from inexpensive starting

material (1,4-naphthoquinone) and the synthetic protocol can be scaled up for a large quantities (5-10 g) without the requirement of cumbersome purification, such as column chromatography. Furthermore, various anionic counter ions of these compounds can be conveniently exchanged to improve the bioavailability.

Previously, we have reported the synthesis of two different sets of CAA's that possess predominately either antibacterial activities or anticancer activities.⁵⁻⁷ The first set of compounds (Figure 1B, left) exhibit strong antibacterial activities against Gram positive (G+) bacteria with minimum inhibitory concentrations (MIC's) lower than 1 $\mu\text{g/mL}$ against *Staphylococcus aureus* (ATCC 25923). The second set of compounds (Figure 1B, right; Scheme 1) exhibit strong anti-cancer activity with GI_{50} values ranging from low μM to nM in the five-dose 60 cell lines assay performed by National Cancer Institute (NCI). By comparison, the first set of compounds only possesses strong antibacterial activity and weak anti-cancer activity; and the second set of compounds exhibit strong anticancer activity and weak antibacterial activity. Synthesis and SAR studies have already been reported for both sets of these compounds.⁵⁻⁷ The SAR study has revealed that an 8-carbon alkyl chain at the 3-N position is the optimum chain length for antibacterial activity; whereas, electron donating group with low steric hindrance at the 3-N aryl group are best group for anticancer activity. More SAR study details are presented in Figure 1B and mode of action study for the first set of antibacterial compounds has been already reported.⁸ Herein, we wish to report the possible modes of action for the second set of compounds that possess anticancer activity.

Several studies have shown that redox cycling properties of quinone are responsible for their anti-cancer activities.^{3,4,9} One electron reduction of quinone forms a semiquinone radical and a

two electron reduction of quinone forms dihydroquinone. Both semiquinone radical and dihydroquinone can be re-oxidized back to their parent quinone by molecular oxygen forming ROS in a redox cycle.¹⁰ The super oxide anions formed during the redox cycle are known to cleave DNA, peptides, and proteins.¹¹ Once cells are unable to repair these damages apoptosis is triggered. The redox cycle can be facilitated by cellular reductases, electron leakage from mitochondria, or another hydroquinone.¹² Our mode of action studies focus on the quantification of cationic 1,4-naphthoquinone analogs induced ROS, oxidative stress, mitochondrial membrane potential, glutathione (GSH) and caspase-3, all of which are related to programmed apoptosis.

RESULTS AND DISCUSSIONS

Cell viability analysis. All the compounds (**1c-9c**) were tested against NCI-60 cell lines and their GI_{50} and LC_{50} values were reported in our earlier publication.⁷ For the purpose of mode of action study, here we chose to study growth-inhibitory effect of compound **2c** on human lung alveolar epithelial cancer cell line (A549) and lung fibroblast cell line (MRC-5) as the control. Various doses of compound **2c** were added to cells for 48 h of incubation and the curve of cell growth was determined by means of 3-(4,5-methylthiazol-2-yl)-2,5-diphenyltetrazolium bromide (MTT) assay. IC_{50} (4.2 μ M) obtained by our experimental conditions are much higher than the GI_{50} (0.34 μ M) value determined by the NCI. The growth media used in our experiment (DMEM 1X) has a higher level of glutathione than the media used by NCI (RPMI), and the higher level of glutathione is believed to be responsible for the observed higher IC_{50} value. Similarly, the IC_{50} value obtained for etoposide is 3.9 μ M (Table 1) for the A549 cell line under similar conditions was found to be at least 4 fold higher than the reported GI_{50} (0.99 μ M) value from the NCI. As shown in Figure 2, compound **2c** exhibits strong cytotoxic effect on the A549

cell line and moderate cytotoxic effects on the MRC-5 cell line. Selectivity is at least 8 fold higher for A549 vs MRC-5 cell line. This selective cytotoxic effect on the assayed cancer cell line greatly enhances the potential of these CAA's as chemotherapeutic agent. As a control experiment, we also tested anticancer activity of antibacterial compound NQM108 on A549 under similar condition as **2c**. The compound showed very low cytotoxicity with IC₅₀ value of 83.33 μ M.

Compound 2c does not affect cell cycle. Many anticancer compounds arrest cells in a certain phase of a cell cycle, for instance cisplatin arrests cells in the G2 phase,¹⁸ doxorubicin arrests cells in G2/M phase,¹⁹ camptothecin arrests cells in the G2 phase²⁰ and some anticancer compounds do not arrest cells at all.²¹ The cell cycle arrest provides some mechanistic information on the mode of action, which makes this assay very important. The cell cycle analysis was carried out after incubation with different concentrations of compound **2c** over 24 h. The cells were then analyzed by flow cytometry. The cell cycle analysis showed no significant effect on any stages of the cell cycles (Figure 5), and the percentage of cells in each phase of cell cycle were not affected by drug concentration. This result also indicates that the mode of action of CAA's are not related to growth and/or growth regulating factors. These compounds are also unlikely to be a topoisomerase inhibitor because all the reported topoisomerase inhibitors (e.g., doxorubicin and camptothecin) are known to arrest the cell cycle at a certain phases. For example, cribrastatin 6 does not affect cell cycle and does not inhibit topoisomerase. Even though compounds arresting the cell cycle are desirable for specific target, they are not very useful for targeting quiescent cells mostly present in tumor.

Compound 2c induces apoptosis in cancer cells. FITC Annexin-V (A)/ Propidium iodide (PI) double staining assay was utilized to study the mode of cell death. The assay takes advantage of the earliest apoptotic process, when phosphatidylserines (PS) from the inner side of the plasma membrane translocate to the outer surface.²² FITC annexin-V is a fluorochrome dye conjugated with Ca^{2+} dependent phospholipid-binding protein with a higher affinity for PS. This high affinity for FITC annexin-V allows detection of early apoptotic cells.²² Once the integrity of the cell membrane is compromised, then PI can get inside the cell and bind with DNA. The level of PI intake directly correlates with the severity of membrane damage. The cells were treated with various concentrations of **2c** (0.0, 0.01, 0.10, 1.0, 10.0, and 100.0 μM) over 24 h and then analyzed by flow cytometry for the cells stained with Annexin-V and PI (Figure 3). Three distinctive populations of apoptotic cells (Gate P12, A^+/PI^- ; Gate 13, A^+/PI^+ ; and Gate P14, $\text{A}^+/\text{PI}^{++}$; Figure 3) were observed. The total number of apoptotic cells increased from 7.70% to 8.74%, 11.06%, 11.07%, 35.44%, and 61.28% at 0.00 μM , 0.01 μM , 0.1 μM , 1.0 μM , 10 μM , and 100 μM concentration of **2c** respectively. The progression of the apoptosis started from healthy cells (A^-/PI^-) to early apoptosis (A^+/PI^-) followed by late apoptosis (A^+/PI^+) and finally necrosis ($\text{A}^+/\text{PI}^{++}$). This process is a very clear indication of cell death via apoptosis. The progression trend of the apoptosis cycle can be observed in the bar diagram (Figure 3). The general morphological characteristics of apoptosis such as cell shrinkage, nuclear condensation, and mitochondrial membrane damage can be observed in Figure 4.

Compound 2c induces oxidative stress by ROS generation. It is well documented that due to rapid metabolic processes, a level of endogenous ROS is elevated in cancer cells compared to normal healthy cells.²³ Further elevation of the exogenous ROS pushes oxidatively stressed cancer cells over a critical redox threshold triggering apoptosis.²⁴ Quinone motif

containing compounds (e.g. adaphostin, menadione, daunorubicin and doxorubicin) are known to kill cancer cells by further elevating ROS level. Selective killing of cancer cells over healthy cells is possible through this pathway by increasing the amount of ROS that pushes cancer cells over their critical threshold, while normal cell lines can survive this ROS level.^{24, 25} The level of ROS production in A549 cells was determined by dichloro-dihydro-fluorescein diacetate (DCFH-DA) dye. The non-fluorescent DCFH-DA dye is cleaved by cellular esterase in the cell which upon oxidation, forms a highly fluorescent adduct. The cells were then analyzed by flow cytometry for any increase in the fluorescence intensity. The incubation of **2c** for 4 h showed correlation between the concentration of compound **2c** and the ROS level (Figure 8). The incubation of **2c** at 10 nM and 100 nM showed no effect on ROS production whereas incubation of **2c** at 10 μ M and 100 μ M showed a significant increase in mean fluorescence. Antibacterial compound NQM108 (Figure 1, left) was also tested for ROS under similar condition. It also generated ROS but the level of ROS was much lower than ROS produced by **2c** (Figure 6, C). The level of ROS considered as 100% at control. At 10 μ M and 100 μ M, NQM108 only increased mean fluorescence by ~108% and ~177% whereas **2c** produced over 133% and 226% respectively. It is likely that cells can cope with the lower level of ROS generated by NQM108 whereas ROS generated by **2c** exceeds the critical threshold resulting in apoptosis.

Compound 2c depletes glutathione in cancer cells. Glutathione (GHS) is a natural antioxidant in many cells. GHS neutralizes harmful ROS produced in the cells. Although the majority of GHS is present in the cytosol, a small percentage of GHS exists in the mitochondria and is critical for cellular functions. Cellular redox processes that take place in mitochondria are vulnerable to the detrimental effect of ROS, and depletion of mitochondrial GHS can have catastrophic consequences. For instance, it has been reported that GHS depletion can serve as a

potent activator of apoptosis signaling.²⁶ The depletion of GHS was measured using glutathione fluorometric assay kit (Biovision, USA). A549 cells were incubated with **2c** for 48 h and the samples were analyzed in a 96 well plate with excitation at 360 nm and emission detection of 460 nm. The level of GHS expressed as 100% for the control, and the decrease in GHS levels after drug treatment was compared to the control (Figure 8). A concentration dependent GHS depletion was observed. Although incubation of **2c** at 0.1 μM only decreased the GHS level to 99.35%, significant GHS depletion was noted at 1 μM and higher concentrations of **2c** with GHS level at 88.76%, 23.87%, and 12.13% after the incubation at 1 μM , 10 μM , and 100 μM of **2c** respectively. This result from GHS depletion assay also supports our earlier results from the ROS assay as GHS depletion elevates ROS level in the cells and vice-versa.

Compound 2c decrease mitochondrial membrane potential. Mitochondria play a key role in activating apoptosis. A decrease in mitochondrial membrane potential ($\Delta\Psi\text{m}$) during apoptosis has been well reported.²⁴ Hence, we decided to examine the effect of **2c** on $\Delta\Psi\text{m}$. A decrease in $\Delta\Psi\text{m}$ leads to matrix condensation and exposure of cytochrome *c* to the intermembrane space, facilitating release of cytochrome *c* into the cytoplasm. This process is facilitated by effectors BAK/BAX oligomerization which form pores in the mitochondrial membrane.²⁷ The release of cytochrome *c* from the mitochondria promotes the activation of the executioner protein caspase cascade. We incubated different concentration of **2c** with A549 cells for 24 h. We used Rhodamine 123 for the $\Delta\Psi\text{m}$ analysis, which distributes electrophoretically into the mitochondrial matrix according to the electric potential distribution across the inner mitochondrial membrane.^{28,29} The intensity of Rhodamine 123 was analyzed by flow cytometry. The experiment showed a concentration dependent change in $\Delta\Psi\text{m}$ even at a very low concentration (10 nM) of **2c**. The gate P4 (Figure 9, A and B) represents the percentage of cells

with decreased $\Delta\Psi_m$. The percentage of cells with decreased $\Delta\Psi_m$ increased from 1.7% (control) to ~2.55% in 10 nM and 100 nM of **2c**. Significant changes were only observed from 1 μM to 100 μM of **2c**. Overall, the percentage of cells which showed a decrease in $\Delta\Psi_m$ increased to 4.10%, 51.40%, and 88.05% at 1 μM , 10 μM , and 100 μM of **2c**, respectively. Under similar condition, NQM108 only increased the percentage of cells with a decrease in $\Delta\Psi_m$ to 25% at 10 μM and 50% at 100 μM (Figure 9, C and D). This data correlates with our earlier ROS result where NQM108 produced a lower amount of ROS than **2c**. The lower amount of ROS damages lower number of mitochondria resulting in fewer cell death. The correlation of these two results clearly explains why **2c** is active and NQM108 is not against cancer.

Caspase-3 release assay. Release of the caspase family of protein is a well-known biomarker for apoptosis via mitochondrial pathway. The release of mitochondrial cytochrome *c* into the cytoplasm activates initiator caspase-8/9. Once activated, they cleave and activate downstream effector caspase-3/-7.³⁰ Caspase-9 activates executioner caspase-3 and caspase-7. They are the executioner proteins which upon activation cleave major cellular components. Caspase-3 is the key player in the digestion of the cellular component, while caspase-7 is responsible for the detachment of apoptotic cells.³¹ Therefore, identification of caspase-3 release is the key final step for the identification of the mode of action from this pathway. Different concentrations of **2c** (0.01 μM , 0.1 μM , 1.0 μM , 10.0 μM and 100 μM) were incubated with A549 cells for 4 h, 12 h, 24 h, and 48 h. The release of caspase-3 was detected by the caspase-3 fluorometric assay kit (Biovision, USA), and analyzed by a 96 well plate reader. The result showed an increase in caspase-3 activity in a concentration and time dependent manner (Figure 10). The highest level of caspase-3 activity was observed when compound **2c** (0.01 μM and 0.1 μM) was incubated with A549 for 24 h. The caspase-3 level had already decreased to the base

level at 10.0 μM . Time dependent release of caspase-3 was also observed at 0.1 μM drug concentration at 4 h, 12 h, and 48 h. The release of caspase family of proteins is a biomarker for mitochondrial dependent apoptosis, hence the increased activities of caspase-3 in our experiment supports the hypothesis that CAA generates apoptosis via mitochondrial pathway.

Due to its structural similarity and redox properties, CAA's are expected to form toxic ROS by hijacking the function of ubiquinone (Q) in the mitochondrial electron transport chain. Having identified ROS generation as the key mechanism, it is crucial to identify the source of ROS. It is well known that ROS are generated by the reduction of molecular oxygen by semiquinone radicals. Semiquinone radicals are formed by one electron reduction of a quinone. The process of formation of semiquinone radical most likely takes place in the mitochondria, where they can hijack the function of electron transporter Q in the electron transport chain. It is well-documented that diverse cationic dyes can readily penetrate the outer membrane of mitochondria and accumulate in the inner mitochondrial membrane electrophorically.^{28, 32, 33} The cationic nature of CAA's may facilitate this accumulation.^{28, 32, 33} Once accumulated in the membrane, CAA's can interfere with the function of ubiquinone due to the similarities in their structure and redox properties. The proposed mechanism is also supported by our previous work where we reported that antibacterial CAA's exert antibacterial activity by inhibiting the redox processes of bacteria.¹⁰ A direct correlation has been reported on multiple heterocyclic quinone's reduction potential and its cytotoxicity.³⁴

The redox potentials of CAA's were determined by cyclic voltammetry (Table 2). All these compounds can undergo redox reactions similar to the inter-conversion of quinones, semiquinone radicals and dihydroxyquinones via a one-electron or two-electron process (Scheme

2). All of the compounds tested exhibited two reversible electrochemical reductions in tetrabutylammonium hexafluorophosphate (TBAF) buffer in anhydrous acetonitrile.

Half wave potentials ($E_{1/2}$) were calculated for all the compounds. We observed that all the active compounds have first $E_{1/2}$ higher than -160 mV; and the less active or inactive compounds have first $E_{1/2}$ lower than -160 mV. The most active compounds with the lowest percentage mean cell growth have greater than -180 mV first $E_{1/2}$. The active compounds contain electron donating groups while inactive compounds contain electron withdrawing groups. The reduction potential of ubiquinone is approximately -556 mV vs Ag/AgCl, -602 vs SCE in aprotic solvent.³⁵ Since the redox potentials of CAA's are much lower than Q, they are much better electron acceptors compared to Q. Thus, it is quite possible that CAA's can replace Q and receive electrons directly from electron-transporting complex (ETC) I or II forming semiquinone radicals (SQR's). It has been reported that SQR's can readily reduce molecular oxygen leading to the formation of ROS. Based on this information, a proposed mechanism is outlined in scheme 3.

The electron withdrawing groups on CAA's can better stabilize the SQR's and slow down the formation of ROS from reduction of molecular oxygen. Whereas, electron donating groups on CAA's can destabilize the SQRs and facilitate the electron transfer to molecular oxygen forming ROS. Although both classes of CAA's can generate ROS, those compounds containing electron donating groups form ROS more rapidly and hence attribute to their higher cytotoxicity. Previously published research also supports this claim where the substitution with electron withdrawing groups on quinone decreases the rate of formation of superoxide while substitution of electron donating groups increases the rate of formation of superoxide.³⁶ Since we only observed a direct correlation between the first half wave reduction potentials ($E_{1/2}$) and anticancer activity, it is likely that these compounds work by one electron reduction at the

cellular level rather than a two electron reduction process, and the redox process between the anthraquinone and semiquinone radicals is responsible for the anticancer activity of CAA's.

CONCLUSION

We have identified the anticancer mode of action of cationic anthraquinone analogs. This mode of action study has revealed that these compounds generate ROS and deplete the natural antioxidant glutathione in the cell. These active compounds possibly hijack the function of ubiquinone due to their similarities in structure and redox properties, thus generating semiquinone radicals. The semiquinone radicals in turn reduce molecular oxygen to form highly reactive ROS. The generation of extensive ROS species and the depletion of the level of glutathione leads to oxidative stress and damage to the mitochondrial membrane lowering its membrane potential. The programmed apoptosis is caspase dependent, and triggered by the release of caspase-3. To unambiguously identify the mode of action, we have performed DNA cleavage and alkylation experiments (please refer to SI for more detail). We have observed direct DNA cleaving capability of these compounds at a higher concentration. Although the DNA cleaving property of CAA's without light and transition metals is very unique to these specific compounds, the DNA cleavage was only observed at much higher concentration than the IC_{50} value, and therefore may not be attributed as the primary mode of action. Other experiments conducted in our laboratory have also ruled out the possibility that CAA's can function as an alkylating agents (please refer to SI for more detail). In summary, our results have confirmed the anticancer mode of action for these novel CAA's and may pave the way for the development of new chemotherapeutic agents.

ASSOCIATED CONTENT

Supporting Information: Final compound purification data; DNA cleavage experiment; alkylation experimental data; and cyclic voltammeter measurements associated with this article.

This material is available free of charge via the Internet at <http://pubs.acs.org>.

AUTHOR INFORMATION

Corresponding Author

tom.chang@usu.edu

* To whom correspondence should be addressed. Ph: (435) 797-3545. Fax: 435-797-3390.

ACKNOWLEDGMENTS

We thank the laboratories of Prof. Takemoto (Department of Biology, USU), Dr. Sanjeev Shrestha (Department of Biology, USU) for providing training and equipments for the DNA cleavage experiments; and Dr. Jianhua Gong (Department of Chemistry and Biochemistry, USU) for mammalian cell related training. We are grateful for the valuable advice from Prof. Rong Wang (Illinois Institute of Technology) regarding the cyclic voltammetry measurements. We also thank National Institute of Antiviral Research, USU for providing A549 and MRC-5 cell lines.

AURTHERSHIP CONTRIBUTIONS

Participated in research design: *Jaya P Shrestha, Yagya Prasad Subedi, Liaohai Leo Chen, and Cheng-Wei Tom Chang**

Conducted experiments: *Jaya P Shrestha and Yagya Prasad Subedi*

Wrote or contributed to the writing of the manuscript: *Jaya P Shrestha, Liaohai Leo Chen, and Cheng-Wei Tom Chang**

FIGURE LEGENDS.

Figure 1: (A) FDA approved quinone motifs containing anticancer drugs; (B) Cationic 1,4-naphthoquinone analogs from our laboratory and SAR summary.

Scheme 1: Synthesis of cationic 1,4-naphthoquinone analogs; Compound **2c** was chosen for mode of action study.

Figure 2: (A) **2c**, NQM108 and etoposide dose response curve for different cell lines.

Table1: IC₅₀ values for **2c**, NQM108 and etoposide against various human cell lines.

Figure 3: Cell cycle analysis for A549 cells incubated with **2c** for 24 h. * = P ≤ 0.05; ** = P ≤ 0.01; *** = P ≤ 0.001; and **** = P ≤ 0.0001

Figure 4: Annexin-V/PI assay for apoptosis. * = P ≤ 0.05; ** = P ≤ 0.01; *** = P ≤ 0.001; and **** = P ≤ 0.0001

Figure 5: (A) Morphological changes in A549 cells treated with **2c**; (B) Morphological changes in A549 cell nucleus and mitochondria treated with **2c**.

Figure 6: Reactive Oxygen production in A549 after incubation of **2c** (A and B), and NQM108 (C) for 4 h. * = P ≤ 0.05; ** = P ≤ 0.01; *** = P ≤ 0.001; and **** = P ≤ 0.0001

Figure7: Glutathione depletion at different time intervals. * = P ≤ 0.05; ** = P ≤ 0.01; *** = P ≤ 0.001; and **** = P ≤ 0.0001

Figure 8: Decrease in mitochondrial membrane potential in A549 cell at different concentration of **2c** (A and B) and NQM108(C and D). * = $P \leq 0.05$; ** = $P \leq 0.01$; *** = $P \leq 0.001$; and **** = $P \leq 0.0001$

Figure 9: (A) Caspase-3 release at different time intervals (1 h, 4 h, 12 h and 48 h); (B) Caspase-3 release at different concentrations (0 μM , 0.01 μM , 0.1 μM , 1.0 μM , and 10.0 μM). * = $P \leq 0.05$; ** = $P \leq 0.01$; *** = $P \leq 0.001$; and **** = $P \leq 0.0001$

Scheme 2: Reaction scheme for formation of semi-quinone and hydroquinone.

Table 2: Redox potentials, antibacterial and anticancer activities.

Scheme 3: Proposed mechanism of ROS formation in ETC by cationic anthraquinone analogs.

REFERENCES

1. D. S. Shewach and R. D. Kuchta, *Chem Rev*, 2009, **109**, 2859-2861.
2. J. W. Lown, *Pharmacol Ther*, 1993, **60**, 185-214.
3. A. B. Pardee, Y. Z. Li and C. J. Li, *Curr Cancer Drug Targets*, 2002, **2**, 227-242.
4. A. D. Bolzan and M. S. Bianchi, *Mutat Res*, 2001, **488**, 25-37.
5. M. Y. Fosso, K. Y. Chan, R. Gregory and C. W. Chang, *ACS Comb Sci*, 2012, **14**, 231-235.
6. J. P. Shrestha and C. W. Chang, *Bioorg Med Chem Lett*, 2013, **23**, 5909-5911.
7. J. P. Shrestha, M. Y. Fosso, J. Bearss and C. W. Chang, *Eur J Med Chem*, 2014, **77**, 96-102.
8. K. Y. Chan, J. Zhang and C. W. Chang, *Bioorg Med Chem Lett*, 2011, **21**, 6353-6356.
9. I. Wilson, P. Wardman, T. S. Lin and A. C. Sartorelli, *J Med Chem*, 1986, **29**, 1381-1384.
10. A. Brunmark and E. Cadenas, *Free Radic Biol Med*, 1989, **7**, 435-477.
11. G. Y. Liou and P. Storz, *Free Radic Res*, 2010, **44**, 479-496.
12. T. J. Monks and D. C. Jones, *Curr Drug Metab*, 2002, **3**, 425-438.
13. N. Kongkathip, S. Luangkamin, B. Kongkathip, C. Sangma, R. Grigg, P. Kongsaree, S. Prabpai, N. Pradidphol, S. Piyaviriyagul and P. Siripong, *J Med Chem*, 2004, **47**, 4427-4438.
14. I. Gomez-Monterrey, P. Campiglia, C. Aquino, A. Bertamino, I. Granata, A. Carotenuto, D. Brancaccio, P. Stiuso, I. Scognamiglio, M. R. Rusciano, A. S. Maione, M. Illario, P. Grieco, B. Maresca and E. Novellino, *J Med Chem*, 2011, **54**, 4077-4091.
15. S. Jimenez-Alonso, H. C. Orellana, A. Estevez-Braun, A. G. Ravelo, E. Perez-Sacau and F. Machin, *J Med Chem*, 2008, **51**, 6761-6772.
16. T. S. Lin, I. Antonini, L. A. Cosby and A. C. Sartorelli, *J Med Chem*, 1984, **27**, 813-815.
17. I. Gomez-Monterrey, P. Campiglia, A. Carotenuto, D. Califano, C. Pisano, L. Vesci, T. Lama, A. Bertamino, M. Sala, A. M. di Bosco, P. Grieco and E. Novellino, *J Med Chem*, 2007, **50**, 1787-1798.
18. P. Jordan and M. Carmo-Fonseca, *Cell Mol Life Sci*, 2000, **57**, 1229-1235.
19. Y. H. Ling, A. K. el-Naggar, W. Priebe and R. Perez-Soler, *Mol Pharmacol*, 1996, **49**, 832-841.
20. Y. P. Tsao, P. D'Arpa and L. F. Liu, *Cancer Res*, 1992, **52**, 1823-1829.

21. M. T. Hoyt, R. Palchaudhuri and P. J. Hergenrother, *Invest New Drugs*, 2011, **29**, 562-573.
22. M. van Engeland, F. C. Ramaekers, B. Schutte and C. P. Reutelingsperger, *Cytometry*, 1996, **24**, 131-139.
23. L. Behrend, G. Henderson and R. M. Zwacka, *Biochem Soc Trans*, 2003, **31**, 1441-1444.
24. E. O. Hileman, J. Liu, M. Albitar, M. J. Keating and P. Huang, *Cancer Chemother Pharmacol*, 2004, **53**, 209-219.
25. D. Trachootham, J. Alexandre and P. Huang, *Nat Rev Drug Discov*, 2009, **8**, 579-591.
26. J. S. Armstrong, K. K. Steinauer, B. Hornung, J. M. Irish, P. Lecane, G. W. Birrell, D. M. Peehl and S. J. Knox, *Cell Death Differ*, 2002, **9**, 252-263.
27. S. Aluvila, T. Mandal, E. Hustedt, P. Fajer, J. Y. Choe and K. J. Oh, *J Biol Chem*, 2014, **289**, 2537-2551.
28. L. B. Chen, *Annu Rev Cell Biol*, 1988, **4**, 155-181.
29. X. Ronot, L. Benel, M. Adolphe and J. C. Mounolou, *Biol Cell*, 1986, **57**, 1-7.
30. M. Brentnall, L. Rodriguez-Menocal, R. L. De Guevara, E. Cepero and L. H. Boise, *BMC Cell Biol*, 2013, **14**, 1471-2121.
31. A. G. Porter and R. U. Janicke, *Cell Death Differ*, 1999, **6**, 99-104.
32. J. C. Smith, *Biochimica et Biophysica Acta (BBA) - Bioenergetics*, 1990, **1016**, 1-28.
33. J. A. Dykens and A. K. Stout, *Methods Cell Biol*, 2001, **65**, 285-309.
34. J. Koyama, I. Morita and T. Yamori, *Molecules*, 2010, **15**, 6559-6569.
35. R. C. Prince, P. Leslie Dutton and J. Malcolm Bruce, *FEBS Letters*, 1983, **160**, 273-276.
36. Y. Song and G. R. Buettner, *Free Radic Biol Med*, 2010, **49**, 919-962.

GRAPHICAL ABSTRACT

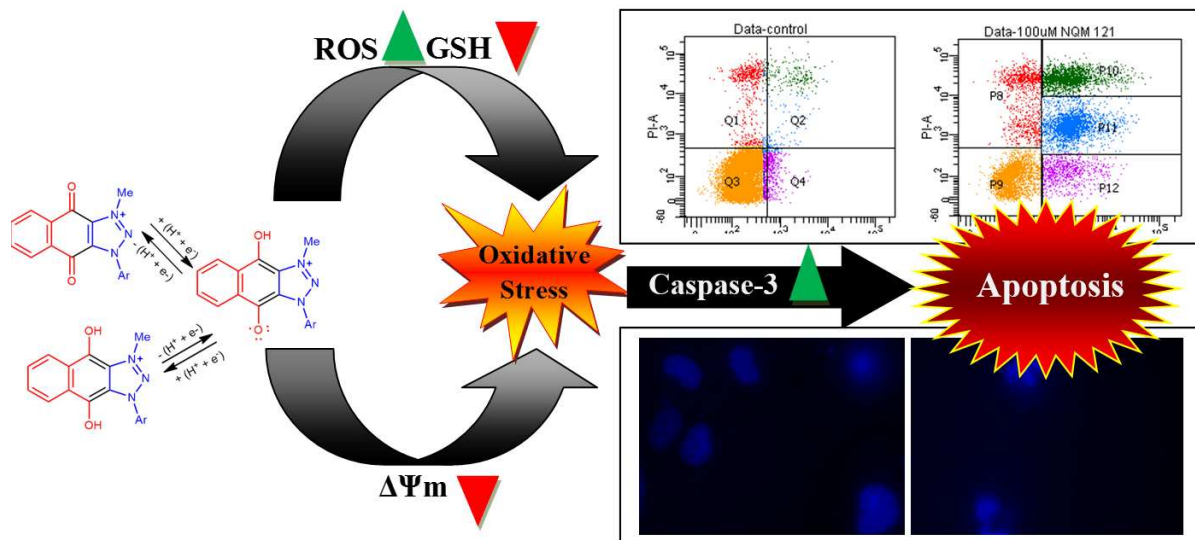
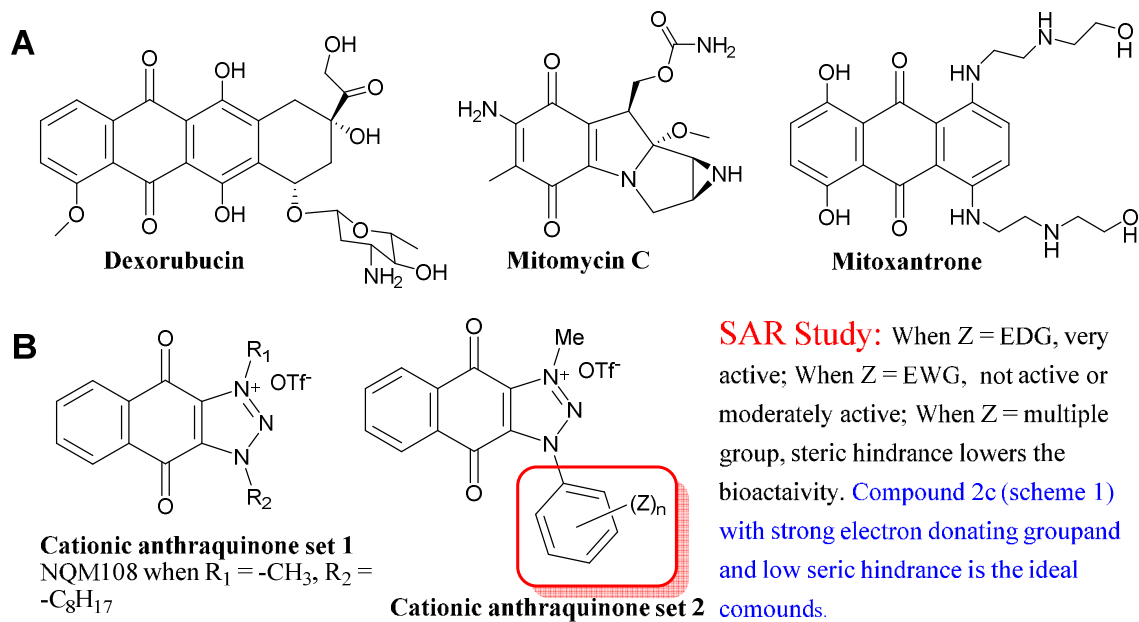


Figure 1:



Scheme 1:

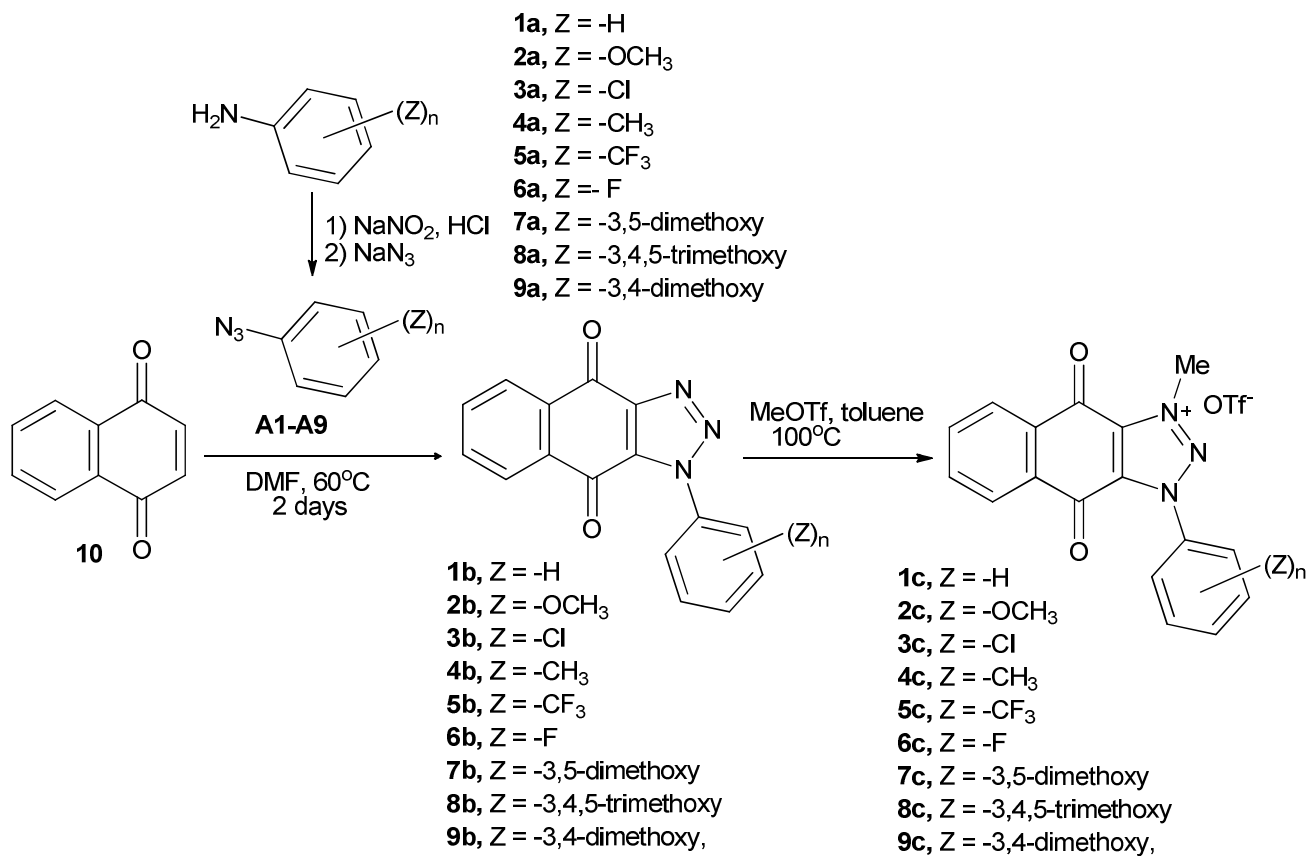


Figure 2:

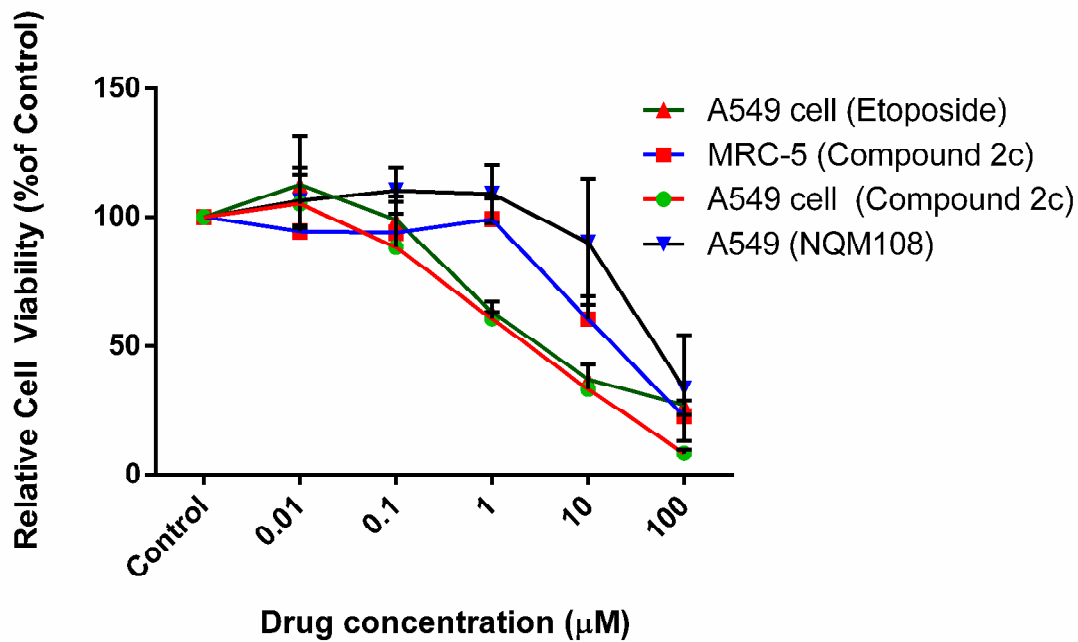


Table 1:

Cell line	IC ₅₀ 2c	IC ₅₀ Etoposide	IC ₅₀ NQM108
A549	4.2 ± 0.5	3.9	83.33±15
MCR-5	35.0 ± 9	-	-

Figure 3:

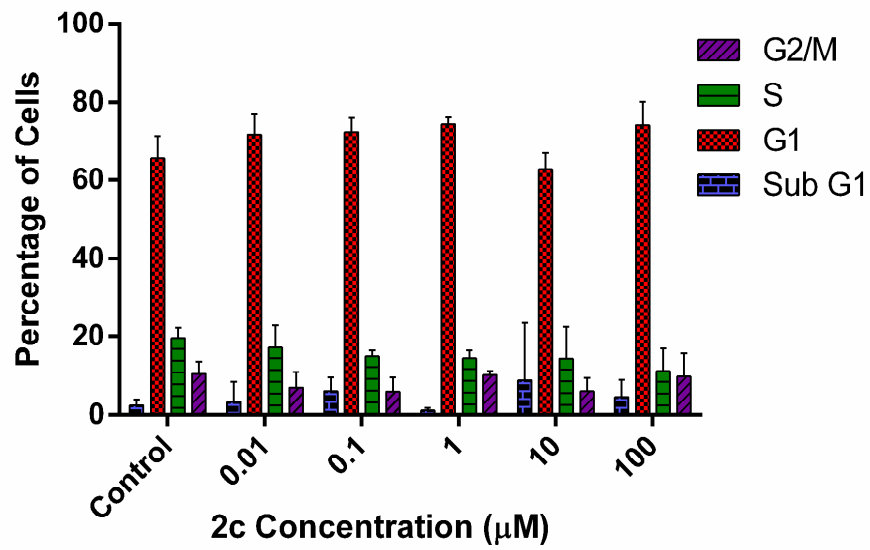
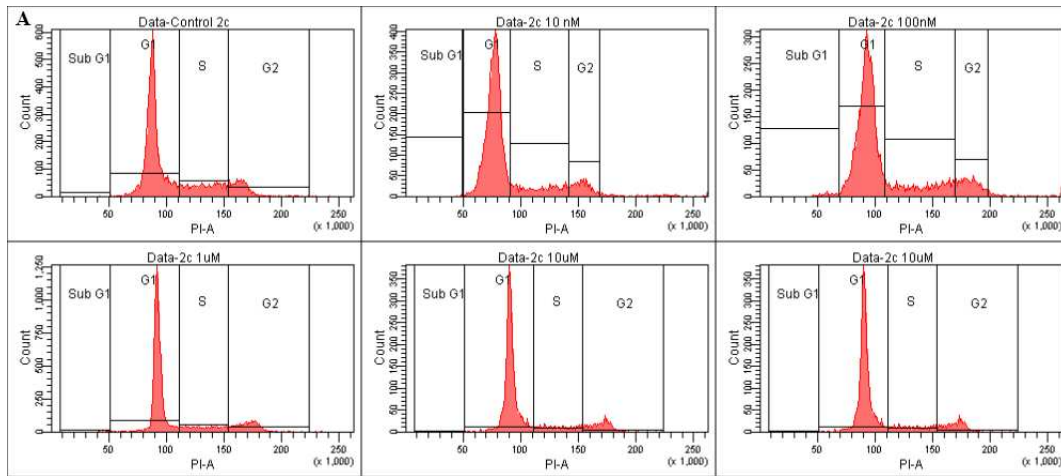


Figure 4:

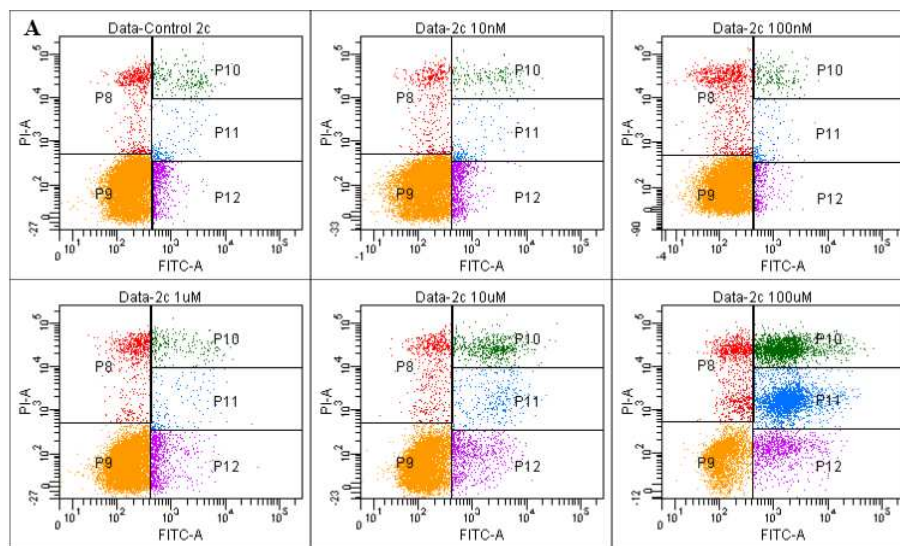
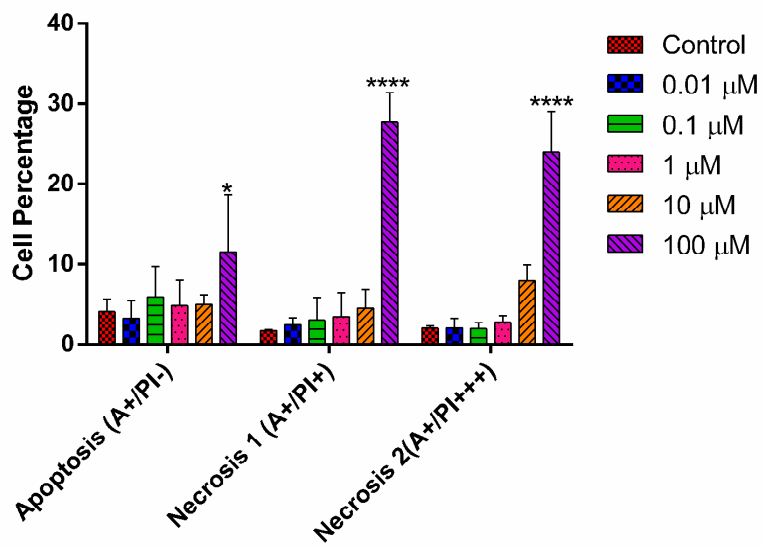
**B**

Figure 5:

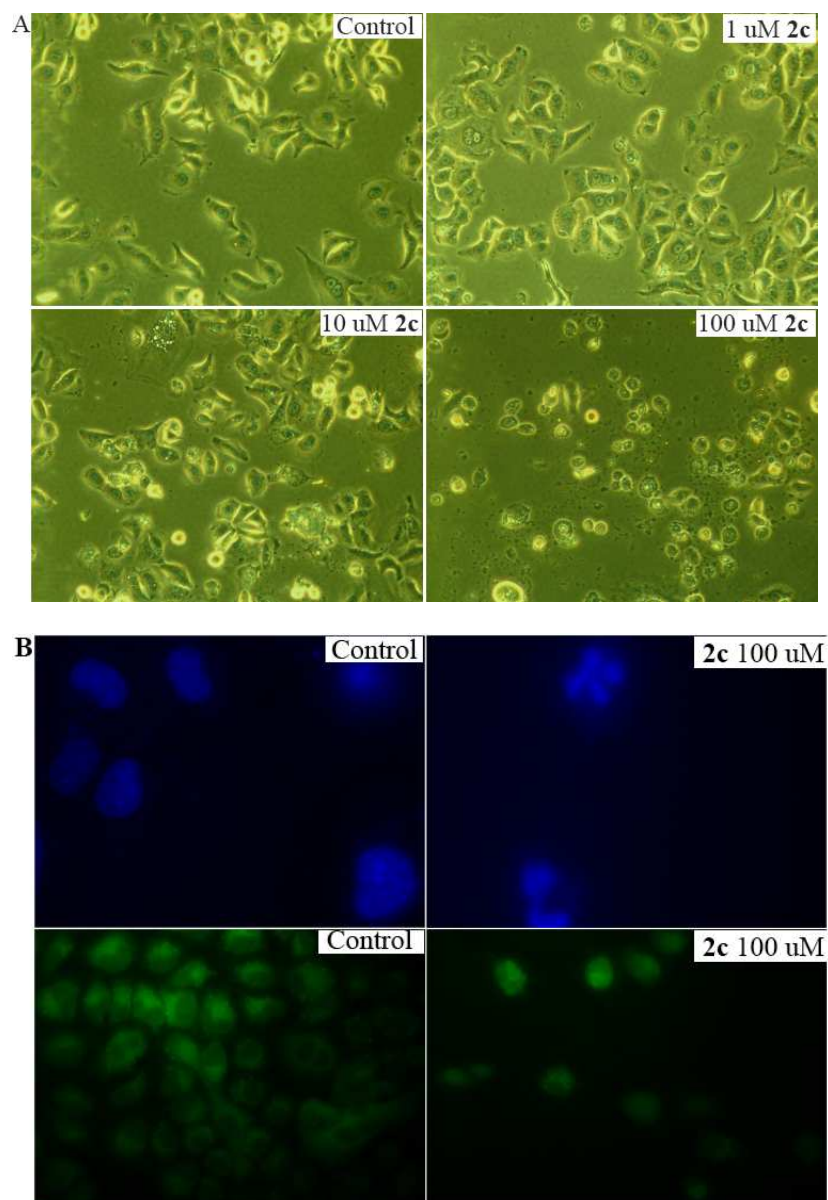
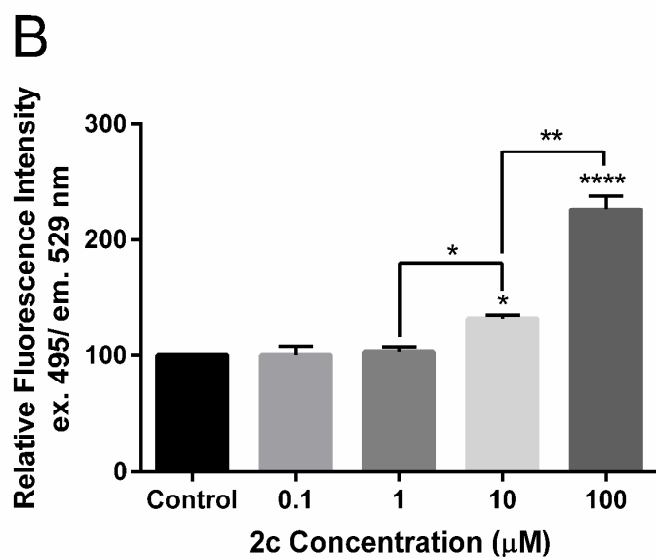
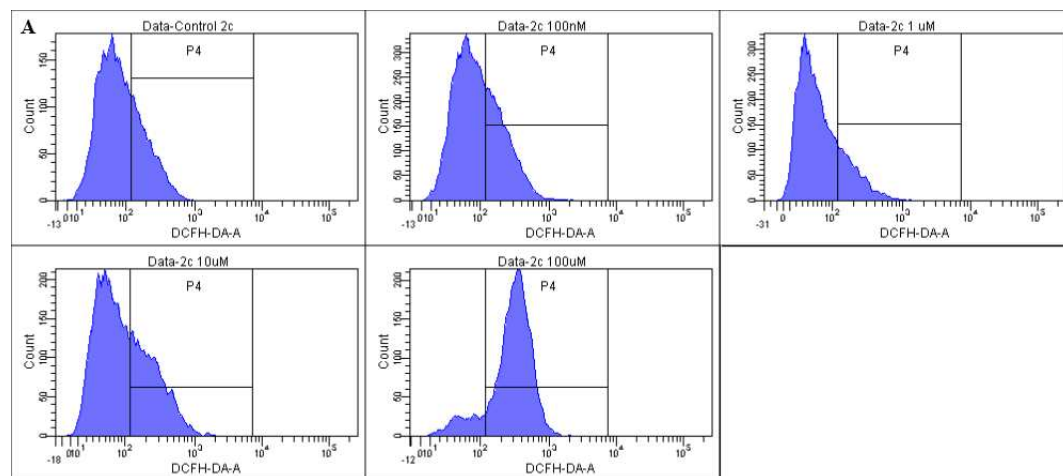


Figure 6:



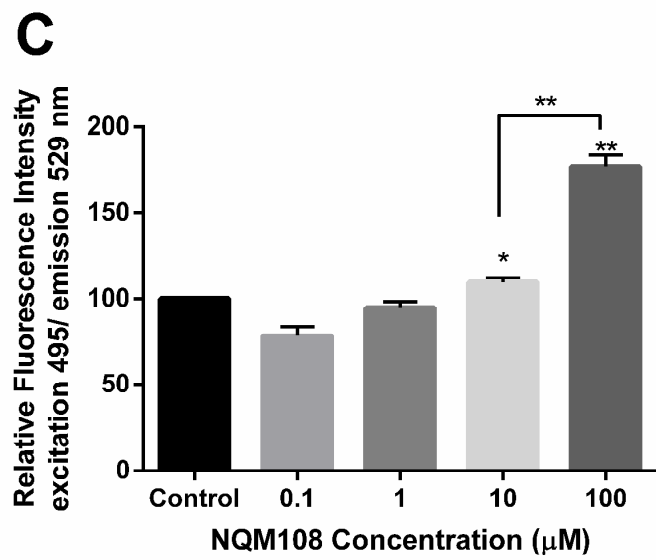


Figure 7:

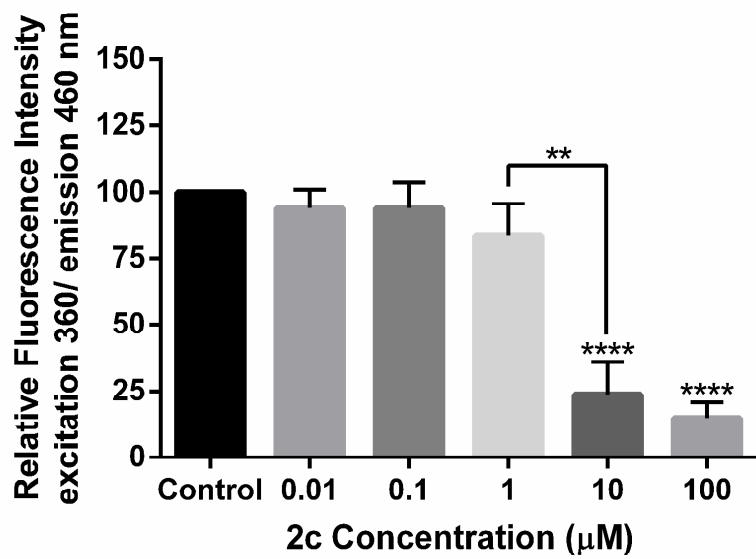
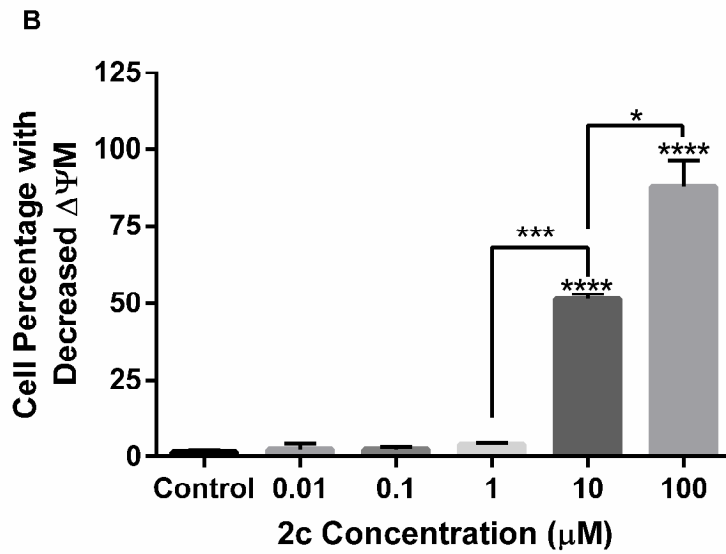
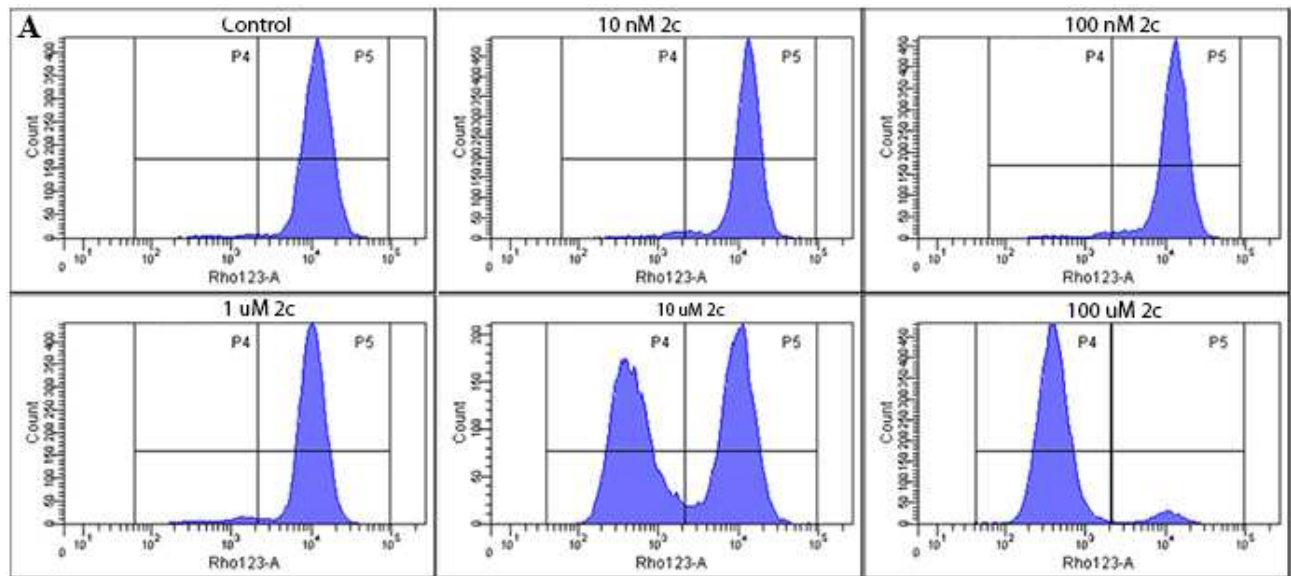


Figure 8:



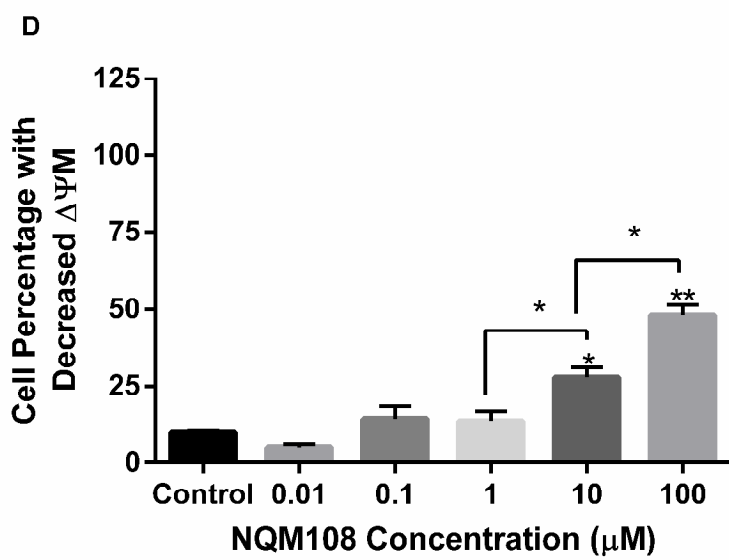
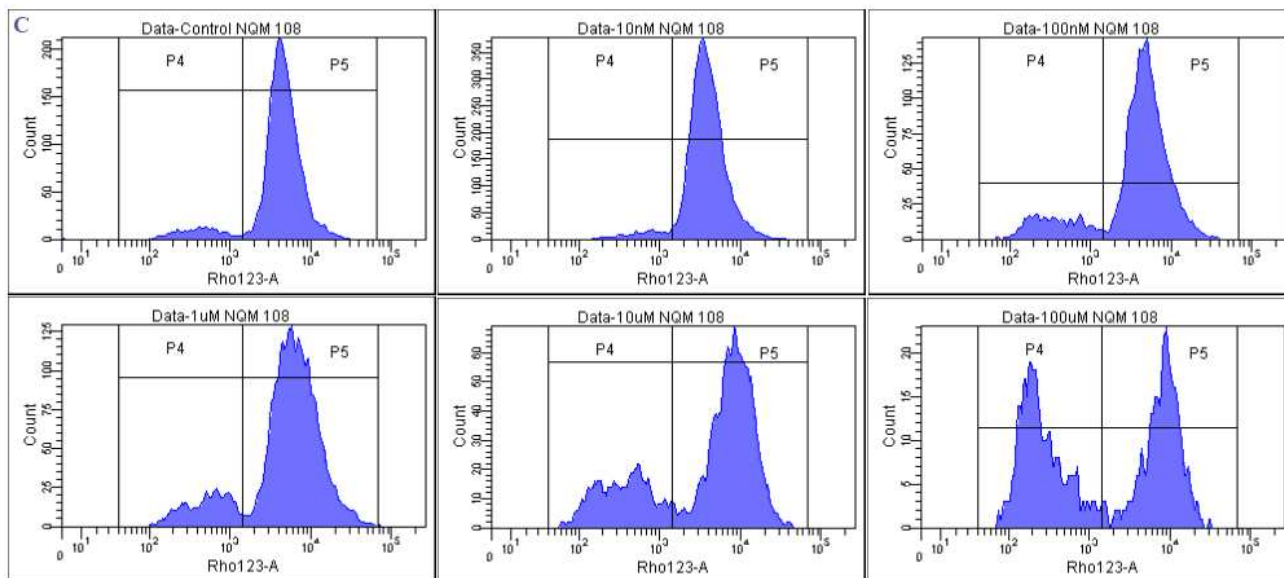
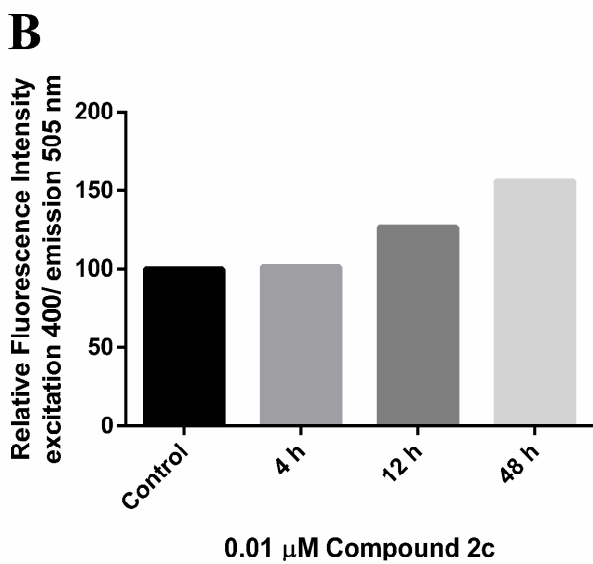
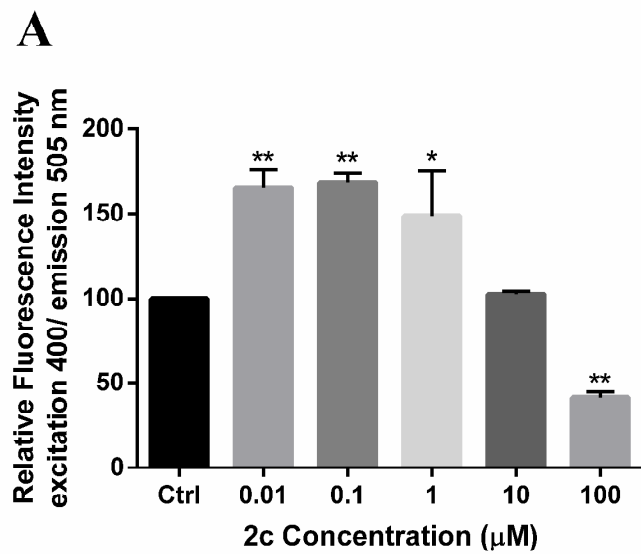


Figure 9:



Scheme 2:

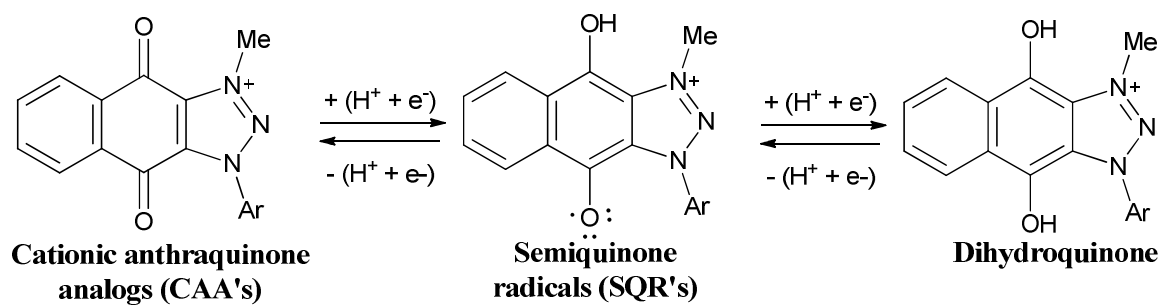


Table 2:

Compound	First wave $E_{1/2}$ (mV) vs (Ag/AgCl, 3M NaCl)	Second wave $E_{1/2}$ (mV) vs (Ag/AgCl, 3M NaCl)	Mean cell growth percentage (%) in NCI- 60 cell line assay
1c	-163.5	-866.5	-10.18
2c	-182.5	-885.0	-24.70
4c	-176.0	-881.5	11.53
5c	<u>-130.5</u>	-823.5	<u>58.69</u>
3c	<u>-148.5</u>	-842.5	<u>101.70</u>
6c	-156.5	-886.0	<u>43.38</u>
8c	-168.0	-867.0	23.23
7c	-182.5	-762.0	-27.06
9c	-182.0	-885.5	-31.51
Ubiquinone	-567 ³⁵	-	-

Scheme 3:

